frontiers | Frontiers in Environmental Science

TYPE Original Research
PUBLISHED 29 July 2025
DOI 10.3389/fenvs.2025.1646182

OPEN ACCESS

EDITED BY
Liu Jibao,
Tokyo Institute of Technology, Japan

REVIEWED BY
Yi Lu,
Guangzhou University, China
Yitian Lu,
Donghua University, China
Yixin Zhang,
Beijing Engineering Research Center of Safety and Energy Saving Technology for Water Supply Network System in China Agricultural University, China

*CORRESPONDENCE
Yanran Zhang,
514342718@shu.edu.cn

RECEIVED 18 June 2025
ACCEPTED 16 July 2025
PUBLISHED 29 July 2025

CITATION
Zang X, Zhang Y and Yue H (2025) Study on the effect of using multi-round citric acid bottom vacuum leaching to remediate Cu, Zn-contaminated soil.
Front. Environ. Sci. 13:1646182.
doi: 10.3389/fenvs.2025.1646182

Study on the effect of using multi-round citric acid bottom vacuum leaching to remediate Cu, Zn-contaminated soil

Xueke Zang[1], Yanran Zhang[2]* and Haofan Yue[2]

[1]Shanghai Yaxin Urban Construction Co., Ltd., Shanghai, China, [2]Department of Civil Engineering, Shanghai University, Shanghai, China

Bottom vacuum-enhanced leaching technology is an effective method for remediation of low-permeability contaminated soil. In order to clarify the influence of drenching rounds on the remediation effect of copper and zinc contaminated soil and soil properties, the change rule of heavy metal removal efficiency and soil properties under different rounds was analyzed through three rounds of citric acid bottom vacuum drenching model test, combined with one-dimensional compression test and microscopic test. The results showed that the leaching rounds had a significant effect. With the increase of the number of rounds, the removal rate of copper and zinc, porosity, permeability coefficient and consolidation coefficient were increased, and the particle size of soil particles was reduced. Microscopically, the structure of the soil samples was looser, and the pore size was enlarged by citric acid corrosion, which promoted the improvement of infiltration and consolidation properties. This study not only elucidated the mechanism of optimizing the pore structure to enhance the remediation effect by washing rounds, but also provided theoretical and technical references for the promotion of the bottom vacuum washing technology and the assessment of geotechnical properties of the remediated soil.

KEYWORDS

contaminated soil, bottom vacuum leaching, leaching rounds, microscopic test, consolidation test

1 Introduction

Soil serves as the foundation for human survival and progress, but the rapid industrialization in the world have led to increasing content of heavy metals in soils, seriously endangering human health and impeding social development. In China, agricultural lands are contaminated by various heavy metals, including Cd, Hg, As, and Cu, among others (Guo et al., 2023). Among the eight heavy metals with the highest concentrations at contaminated sites, Cu and Zn contamination levels are second only to Cd and Pb (Yan et al., 2022) and have become the keywords in the study of polluted sites (Shentu et al., 2023).

For a long time, experts and scholars have conducted significant research on the remediation of heavy metals contaminated soil, among which leaching remediation is known for its cost-effectiveness, efficiency, and ability to permanently remove heavy metals (Antoniadis et al., 2017; Zheng et al., 2022). The agents commonly used in leaching remediation are organic acids, like citric acid (CA), which can form soluble complexes with heavy metals (Liu et al., 2023). Citric acid is self-degradable, does not damage soil structure,

and is considered an environmentally friendly agent, which, combined with its excellent cost-effectiveness, makes it a popular choice for leaching remediation (Chen et al., 2016). The Zn content decreased significantly after leaching with citric acid and water-soluble chitosan (WSCS) (Hu et al., 2021). However, remediation requirements are sometimes not met after a single round of citric acid leaching, the removal rates of heavy metals were only 14.2% and 41.7%, respectively (Ke et al., 2020). In addition, for low-permeability soils with more than 30% clay content, the intergranular structure is congested, making leaching agents difficult to pass through (Rehman et al., 2023). Meanwhile, due to the clay minerals, soils show more significant adsorption and fixation of heavy metal ions, which ultimately results in the inefficiency of traditional chemical leaching method (Zaki et al., 2017; Cyriac et al., 2024; Covelo et al., 2007; Novikau and Lujaniene, 2022; Li et al., 2023; Xu et al., 2017). In response to such cases, numerous studies have shown that the combination of prefabricated vertical drains with vacuum preloading foundation improvement techniques can improve the remediation efficiency and reduce the remediation time for contaminated soils (Liao et al., 2022; Saowapakpiboon et al., 2011; Indraratna et al., 2016; Tang and Shang, 2000; Indraratna et al., 2004; Lei et al., 2017; Liu et al., 2018). The latest bottom vacuum leaching method greatly improved the removal rate in contaminated soil, reduced leaching time, and was also suitable for silty clay (Wu et al., 2022b).

The cumulative number of contaminated sites treated in China in the last decade reached 537. With the expansion of cities in our country, these remediated sites are bound to face reuse, so investigation and evaluation of the restoration effect of remediated sites are needed (Liu et al., 2021; Rehman et al., 2023). Regarding curing/stabilization remediation techniques, soils' pH and unconfined compressive strength increased significantly after curing agent treatment (Rehman et al., 2023). For soil leaching, the pH, TN (total nitrogen), AP (available phosphorous), and enzyme activity of soil significantly decreased after acid leaching (Wang et al., 2020), and too high a concentration of leaching agent led to acidification (Han et al., 2024).

In a context where a large number of industrial lands might transition into construction lands, the soil environment has a strong influence on the soil characteristics (Zhang X. et al., 2022), including the shear and microscopic properties of the soil (Sheng et al., 2025). The impact of citric acid leaching rounds on the soil environment after leaching is not yet clear. In particular, it has been noted that excessive leaching can lead to soil acidification, increased carbon emissions and poorer bio-friendliness. This directly relates to the potential reuse and recovery of sites contaminated with heavy metals. Therefore, it became necessary to study the influence of leaching rounds on the remediation effect and geotechnical properties (Raza et al., 2021; Kuśmierz et al., 2023). It is established that employing bottom vacuum leaching can effectively remediate low-permeability polluted soil (Wu et al., 2022a; Wang et al., 2024), but this technology is prone to causing drainage pipe blockages (Zhang et al., 2025), which reduces the effectiveness of repairs and leaves room for improvement, this paper will explore the remediation effect of multi-round leaching bottom vacuum enhancement on heavy metal-contaminated soil. In addition, we will change the single dimension of the past research and reveal the remediation mechanism from the macro and micro perspectives. Soil column leaching model bucket tests with different rounds of citric acid leaching (one, two and three rounds) will be set up, and the leached soil samples will be subjected to a heavy metal concentration test, consolidation test, particle analysis test, scanning electron microscope (SEM) test, and X-ray diffraction (XRD) test. This paper will directly evaluate the impact of the washing rounds from multi-dimensions, and provide multi-dimensional theoretical support for the subsequent improvement of contaminated soil remediation effects and technology refinement.

2 Materials and methods

2.1 Soil samples

2.1.1 Pre-treatment of soil samples

The test soil samples were obtained at a depth of 2 m from a project on Chuansha Road in Pudong New Area, Shanghai. By testing, the soil is clay, and the particle content of less than 0.075 mm is more than 90%, of which the clay content is more than 30%. The soil specific gravity is 2.67, the plasticity index is 23%, organic matter content was 2.65%, and the pH value is 7.9. After transporting the collected soil samples to the laboratory, air dried naturally, removing obvious garbage such as leaves and plastic bags. Then dried in a constant temperature drying box at 75°C and sieved by 2 mm. The preparation process is shown in Figure 1.

2.1.2 Contaminated soil preparation

According to the standard of Soil Environmental Standard (GB15618-2018), $CuSO_4{\cdot}5H_2O$ and $ZnSO_4{\cdot}7H_2O$ were added to the soil, so that the concentration of Cu and Zn exceeded the standard value by two four times, both of which were 1,000 mg kg^{-1}. Then, add deionized water until the soil is saturated to form 50% soil moisture content, and stir well. To fully adsorb heavy metals, the soil was cultivated in a constant temperature and humidity environment for 1 month, at which point adsorption equilibrium is reached (Kamal et al., 2021).

To detect the soil samples' heavy metal content before and after pollution, the inductively coupled plasma (ICP) test method was used. The original soil samples were found to have very low Cu and Zn content, 30.1 ± 5.7 mg kg^{-1} and 142.3 ± 8.9 mg kg^{-1}, respectively. After 1 month of contamination, the Cu and Zn concentrations were 967.1 ± 20.5 mg kg^{-1} and 1139.4 ± 31.2 mg kg^{-1}, which basically reached the 1,000 mg kg^{-1} concentration requirement set for the test, and the leaching test could be started.

2.2 Soil column leaching test and test methods

In this paper, the one-dimensional compression characteristics of the soil after different rounds of citric acid leaching were investigated based on the bottom vacuum leaching restoration technique. Three model buckets were set up to apply citric acid leaching for one round (CA-round 1), two rounds (CA-round 2), and three rounds (CA-round 3), respectively. The optimal experimental parameters were selected, according to the relevant tests, the optimum pressure value is obtained at this time, the pressure value was kept at 60 kPa (Wu et al., 2022a), the solid-liquid ratio was 1:2 (kg L^{-1}), and the concentration of citric acid

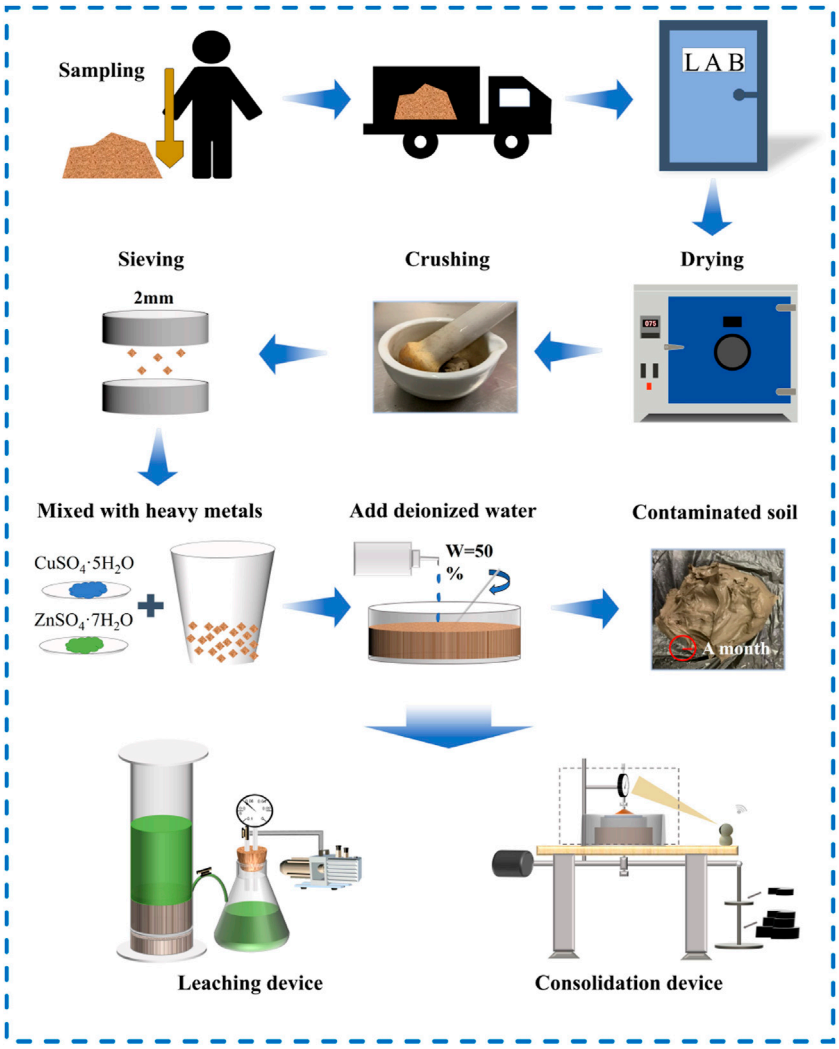

FIGURE 1
Flow diagram of the experiments.

was 0.1 mol L^{-1}, which were the optimized parameters (Wu et al., 2022a; Ke et al., 2020).

The soil column leaching device included model buckets, agent collection bottles, regulators, pressure valves, pressure monitors, an air compressor, and plastic tubing connecting each device. Each model bucket was 50 cm tall with an inner diameter of 13 cm and a 1 cm hole at the bottom. The hole was connected to a plastic tubing outside and a drainage board inside. The top of the drainage board had a 3 cm thick sand cushion covered by a geotextile. Above the geotextile was the contaminated soil, followed by the leaching agent. The test was equipped with collection bottles for collecting and recording the volume of leachate. The vacuum and negative pressure values of the four groups of tests were kept constant by the pressure valves, which control the tests beginning and end. Figure 1 shows the leaching device. Prior to the test, each model bucket was loaded with 1.5 kg of contaminated soil with 50% moisture content (1 kg dry weight). Each round prepares 2L of citric acid solution and adds it above the soil column. At the end of a round of testing, repeat the process with fresh agent. The absence of a significant solution above the soil column is considered to be the end of leaching. The total time consumed for CA-round 1, CA-round 2 and CA-round 3 of tests were 215, 528 and 692 h respectively. Although the total time of the experiment gradually increased, it was not proportional to the increase in the number of leaching rounds. CA-round 2 was 311h longer than CA-round 1, and CA-round 3 was only 164h longer than CA-round 2.

After three model buckets washing tests were completed, the soil column was taken out and uniformly divided into three parts: top, middle and bottom according to height, to compare the difference in the washing effect of soil samples at different heights. Each section is subjected to heavy metal concentration tests, one-dimensional consolidation tests, particle analysis tests, SEM and XRD. Three groups of samples were taken for each part, and the average concentration was taken by repeated detection using ICP (PERKINE 7300DV). The one-dimensional consolidation test is carried out by stacking or inverted sample method, a triple medium voltage reinforcing device (model WG) from Wuxi Xinjian Instrument Technology Co., Ltd. was used, consolidation devices is shown in Figure 1. After the consolidation test was completed, the SEM and XRD test results were obtained by a Japanese electron scanning electron microscope (JSM-IT800) and a multifunction X-ray diffractometer

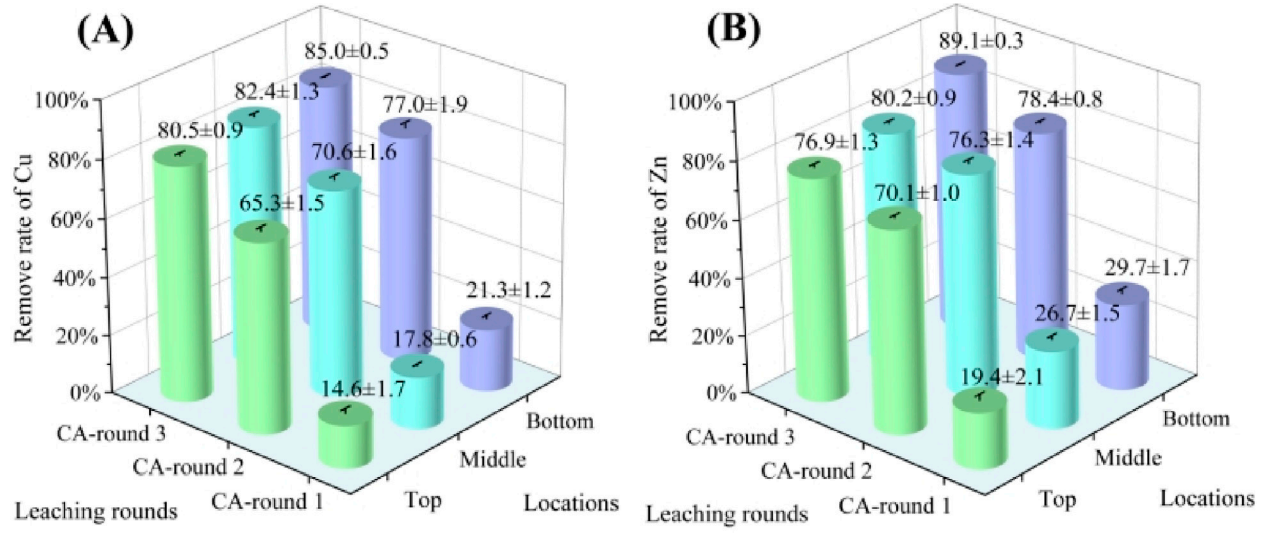

FIGURE 2
(A) Removal rates of heavy metals copper by citric acid treatment with different leaching cycles, **(B)** Removal rates of heavy metals zinc by citric acid treatment with different leaching cycles.

(3KWD/MAX2200V). To obtain the soil particle composition more accurately, this paper uses the BT-9300ST laser particle size analyzer to carry out the particle gradation test (whose significant advantage is that it can get the colloidal content and analyze the soil from the microscopic perspective). At the end of the test to prevent environmental contamination of the drench, $Ca(OH)_2$ was used and the pH was adjusted to 8–10. The carboxyl group of citric acid dissociates under alkaline conditions, thus breaking the chelating bonds with Cu^{2+} and Zn^{2+} and releasing the metal ions to form the hydroxide precipitates $Ca(OH)_2$ and $Zn(OH)_2$.

3 Results

3.1 Heavy metal removal effect

3.1.1 Heavy metal removal rate

The removal rate of heavy metals is a fundamental consideration in the study of remediation effectiveness. The calculation equations are shown in Equations 1, 2.

$$M_{hm} = M_s \times B \tag{1}$$

$$W = \frac{(B - N) \times M_s}{M_{hm}} \times 100\% \tag{2}$$

N-Cu, Zn mass ratio after leaching (mg kg^{-1});
M_s-Soil mass (kg);
M_{hm}-Total Cu and Zn (mg);
B-Cu, Zn mass ratio (mg kg^{-1});
W-Heavy metal removal rate (%).

Due to the non-homogeneity of the soil, the soil samples had different internal leaching orifices and different contact times with the leaching solution, resulting in slight differences in heavy metal removal rates at different locations in the same soil layer. Figure 2 shows the average removal rate and its standard deviation for each location of the three model buckets. The average difference in the removal rate between CA-round 1 and CA-round 2 was more than 50%, and the difference between CA-round 2 and CA-round 3 was about 10%, which strongly supported the conjecture that a large number of citric acid molecules in CA-round 1 of leaching failed to take part in the reaction with the heavy metals, but were degraded by soil microorganisms (Wang et al., 2020; Li et al., 2018). The highest Cu and Zn removal rates were all in the bottom part of CA-round 3, reaching 85.0% ± 0.5% and 89.1% ± 0.3%, respectively. In CA-round 2, Cu and Zn removal rates reached 77.0% ± 1.9% and 78.4% ± 0.8%, removing most of the heavy metals. The addition of one leaching cycle extended the treatment duration by 164 h, yet only resulted in marginal improvements of 8.0% and 10.7% in heavy metal removal rates. This demonstrates that after CA-round 2, further time increases show no significant enhancement in heavy metal removal efficiency. Moreover, each additional leaching cycle doubles the consumption of cleaning chemicals. Considering economic factors, CA-round 2 is sufficient to meet remediation requirements for contaminated soil.

In addition, there was a clear pattern of removal rates between locations - the closer to the bottom, the higher the removal rate. The reason was that citric acid could effectively remove heavy metals from the surface of soil particles in the top and middle sections, but these metals remained in the pore fluid due to the poor drainage condition, and were not wholly removed, causing a low removal rate. On the contrary, the bottom drains quickly and has a high removal rate.

3.1.2 Mechanism analysis

The reaction mechanism is shown in Figure 3. Citric acid is a low molecular weight organic acid that is a natural complexing agent, that can ionize three H^+ in water. The hydrogen ions could, on the one hand, undergo an ionic replacement reaction with Cu^{2+} and Zn^{2+} adsorbed on the surface of soil particles, so that the Cu^{2+} and Zn^{2+} were free in the pore liquid, and the diffusion electric double

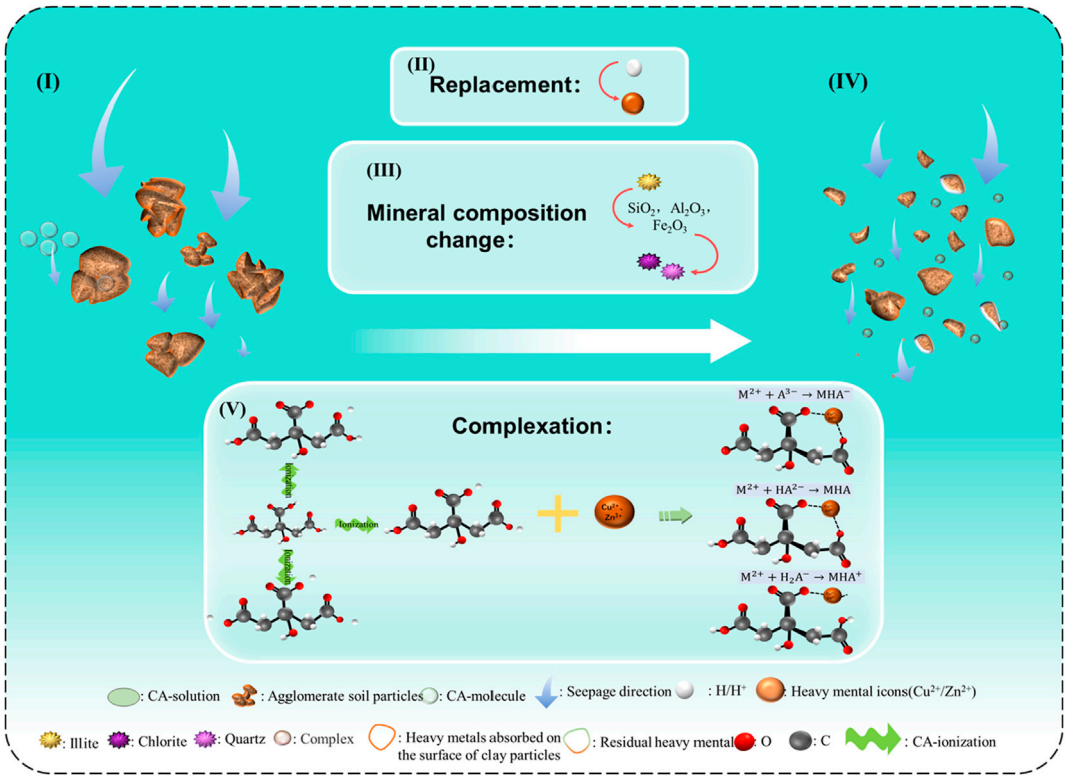

FIGURE 3
Schematic diagram of the leaching mechanism.

layer of the polluted soil particles thickened in the process of replacement, which further led to the disintegration of agglomerates (Xie et al., 2021), and, on the other hand, provided an acidic environment for the leaching to make the mineral compositions change (Liu et al., 2023), as shown in Figure 3 (II) (III). Cu^{2+} and Zn^{2+} free in the pore liquid would interact (complexation) with another product (HA^{2-}, A^{3-}, H_2A^{-}) produced by citric acid ionization to form a water-soluble complex, and the water stability of the complexed product was MHA^{-}>MHA>MHA^{+} (Ke et al., 2020). The complexation process and the equation are shown in Figure 3 (V). At the same time, the acidifying effect of citric acid weakens the electrostatic attraction between soil particles, which leads to the disintegration of agglomerates, which is manifested as an increase in the percentage of clayey grain content. At this point the soil compression coefficient increases, the pore ratio rises and permeability is enhanced. This structural change has a positive effect on heavy metal removal, and the elevated pore connectivity accelerates the infiltration and diffusion of the citric acid solution, resulting in fuller contact between heavy metals and citric acid.

3.2 Consolidation and compression characteristics of remediated soil

3.2.1 Pore and permeability characteristics

Figure 4 reveals the effect of different leaching rounds with citric acid on porosity and permeability coefficient. It is visible that the curves shift upward, indicating that the porosity gradually increases from CA-round 1 to CA-round 3. By observing the decreasing curves of void ratio in Figures 4A, B, there were two stages according to changes: the stage I (0–100 kPa), the porosity decreases by more than 70% rapidly. In this stage, the top and middle soil mainly drained the free water.

The second II (100–800 kPa) for the void ratio change was gentler; the top and middle soil samples in this stage were discharged of pore-free water post a certain consolidation degree, with the soil skeleton mainly bearing the upper load (Liu et al., 2023), resulting in the compression of the pores in the particles. In Figure 4C, the cut-off point between the two phases was the vertical load of 200 kPa, which was due to the more obvious influence of the vacuum load on the bottom soil, which gave the soil a certain consolidation yield pressure (Hong et al., 2010), so that the decline stage of the void ratio was extended. Overall, the porosity was positively correlated with the number of leaching rounds. Still, the distribution pattern of the pore development in the soil remained unchanged.

The variation of the permeability coefficient with pressure for different leaching rounds is given in Figures 4D–F. Similarly, the curve could be divided into three phases.

In Stage I (0–100 kPa), the permeability coefficient declined rapidly with the vertical load.

In Stage II (100–400 kPa), the permeability coefficient declined slowly. Within this stage, the difference between different leaching rounds at the same location was more apparent. The reason for this is that as the number of leaching rounds increased, the remove rate increased and the diffuse double layer of fine particles is subsequently thickened (Li et al., 2015), the free water was

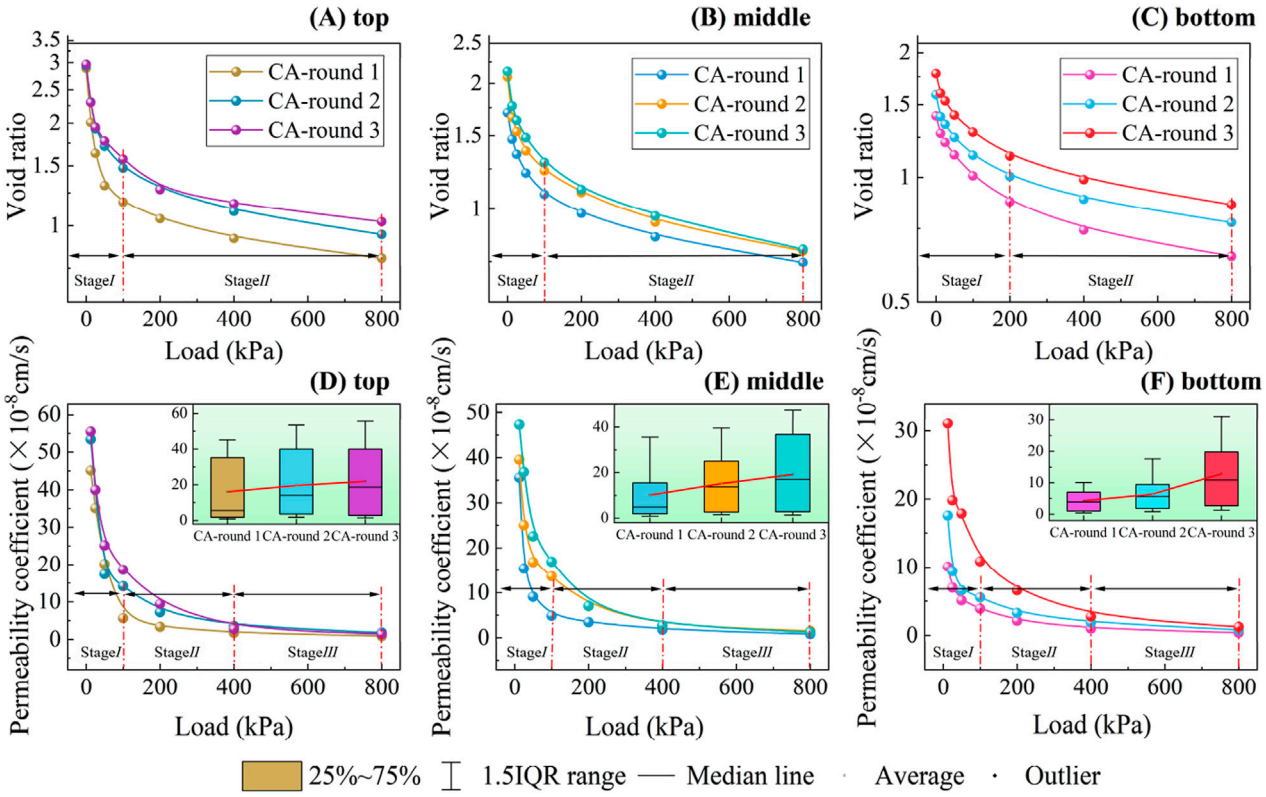

FIGURE 4
Variation with load at the same location for different leaching rounds ((**A–C**) void ratio; (**D–F**) permeability).

conversed to bound water. Only 10%–20% of the heavy metals were removed in CA-round 1, leading to a smaller diffusion electric double layer thickness, more significant effective void, and higher drainage efficiency compared to subsequent rounds, so the infiltration coefficient of CA-round 1 had the smallest change by the second stage. In contrast, CA-round 2 and CA-round 3 achieved heavy metal removal rates exceeding 70%, causing bound water clearly increased. At the same time, the inter-particle distance decreased significantly after the first stage, amplifying the effects of diffusion electric double layer thickness and bound water content on the permeability coefficient (Zhang J. et al., 2022). Consequently, after the considerable reduction of free water in the first stage, CA-round 2 and 3 still needed to discharge more bound water and some free water than CA-round 1 in Stage I. This resulted in a more pronounced decrease in the permeability coefficient of CA-round 2 and 3 in stage II, with a gradual increase in the slope.

Stage III (400–800 kPa), the permeability coefficients exhibited a slight decrease, which was related to the porosity reduction caused by the dislocation of the chimeric soil particles that made up the soil skeleton (Yu et al., 2022; Kwangkyun et al., 2013). The box plots in Figures 4D–F are statistically analyzed for the permeability coefficient, with the middle line being the average line. Obviously, increasing leaching rounds contributes to a larger average permeability coefficient. The middle and bottom soil samples experienced a noticeable increase in box volume indicating that multiple leaching of soil samples had a large impact on the middle and bottom soil.

3.2.2 Consolidation and compression characteristics

In engineering practice, a constant coefficient of consolidation is usually used for settlement calculations (Zuo et al., 2024); however, numerous researches indicated that the coefficient of consolidation changes constantly during soil compression (Elkateb, 2017; Mejlhede et al., 2023; Cui et al., 2023). Similarly, in Figures 5A–C that with the increase in the amount of citric acid leaching, the soil's consolidation coefficient curve shifted upward, and the consolidation coefficient increased gradually. The most significant changes were observed during CA-round 1 to CA-round 2, especially in Figure 5C, where the consolidation coefficient increased by more than twice. This is due to the high porosity, the dispersed particles and the fragile soil skeleton structure caused by the multiple leaching rounds, which is more susceptible to compression.

In Figures 5D–F he compression coefficient curve of the soil shifted upward, indicating a gradual increase in compression coefficient with each additional round of citric acid leaching. This was particularly evident in Figure 5D, where the compression coefficient after three rounds of leaching in the stage I increased by about 87% compared to the first round. The reason is similar to the consolidation coefficient, related to porosity and particle variations (Lin et al., 2022).

The compressive modulus of each test group is shown in Figures 5D–F, which are inversely proportional to the compression coefficients. The overall compression modulus gradually

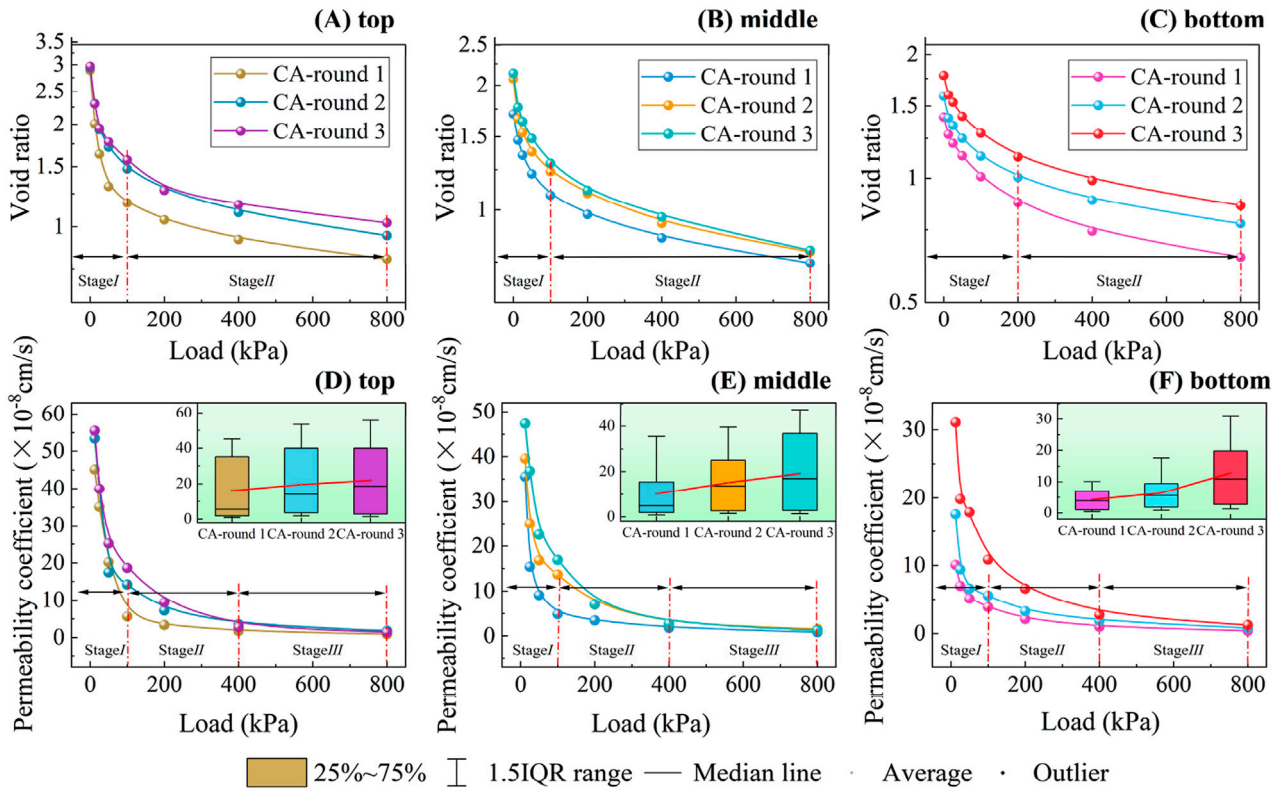

FIGURE 5
Variation with load at the same location for different leaching rounds ((**A–C**) consolidation coefficient; (**D–F**) compression coefficient).

decreased with leaching rounds increasing. It is well known that the compressibility of the soil skeleton is related to its particle composition, bound water content, the thickness of the double electric layer, and other micro-physical and chemical properties (Jongkwan et al., 2021; Aria et al., 2022; Oliveira and Massao, 2015; Hao et al., 2022; Wu et al., 2023). Overall, as the soil particles interact with citric acid in different rounds changes the microscopic properties of the soil considerably, in turn, affects the engineering properties of the soil.

3.3 Microscopic characteristics of remediated soil

3.3.1 Particle size distribution

Figure 6 compared the particle distribution of different leaching rounds at the same location, and observed the effect of the leaching round on soil particle movement. Figures 6A–C corresponded to the top, middle and bottom layers of the soil sample, respectively. The particle composition changed continuously with the increase of the leaching rounds, and the local enlarged images showed the cumulative particle content at the 0.005 mm (clay) position. It can be found that the clay content at the top was CA-round 1 > CA-round 2 > CA-round 3, while the bottom showed the opposite pattern, indicating that the migration movement of clay particles gradually intensified with the leaching rounds, and more clay particles migrated to the bottom. The clay content in the middle part shown in Figure 6B was CA-round 3 > CA-round 1 > CA-round 2, which was due to the increase of porosity from CA-round 1 to CA-round 2, the top and middle clay particles migrated a large amount to the bottom part under the action of pore fluid (Yang et al., 2023). The migrating clay content was greater than the clay content decomposed by large particles, so that the overall clay content decreased (Jez and Lestan, 2016). From CA-round 2 to CA-round 3, the effect of the agent was more obvious, the particle decomposition produced vast clay particles, and the top clay particles migrated to the middle part and could not be discharged in time, so the clay content in the middle part increased, exceeding the initial content.

Figure 6D showed the composition of soil particles in different locations after CA-round 3, it can be seen that clay content was bottom> middle > top. Because the bottom drainage board was the destination of clay migration, the clay particles converged downward after 3 leaching rounds, with the greatest clay content near the bottom drainage board.

3.3.2 Microstructure

The microstructures of the soil samples with different leaching cycles and the original contaminated soil samples at magnifications of 400, 1,000, 2,000 and 5,000 are presented in Figure 7. In Figures 7A, B, compared to the original contaminated soil, the soil samples in CA-round 1 showed a decrease in the aggregates size. As leaching cycles increased, Figures 7C, D depict a gradual loosening of the microstructure. The surface of the soil samples was relatively flat, with a significant reduction in folds, an increase in surface-to-surface contact, and a pronounced macroporous structure, which is consistent with the results of the pore ratio tests. In Figures 7E–L,

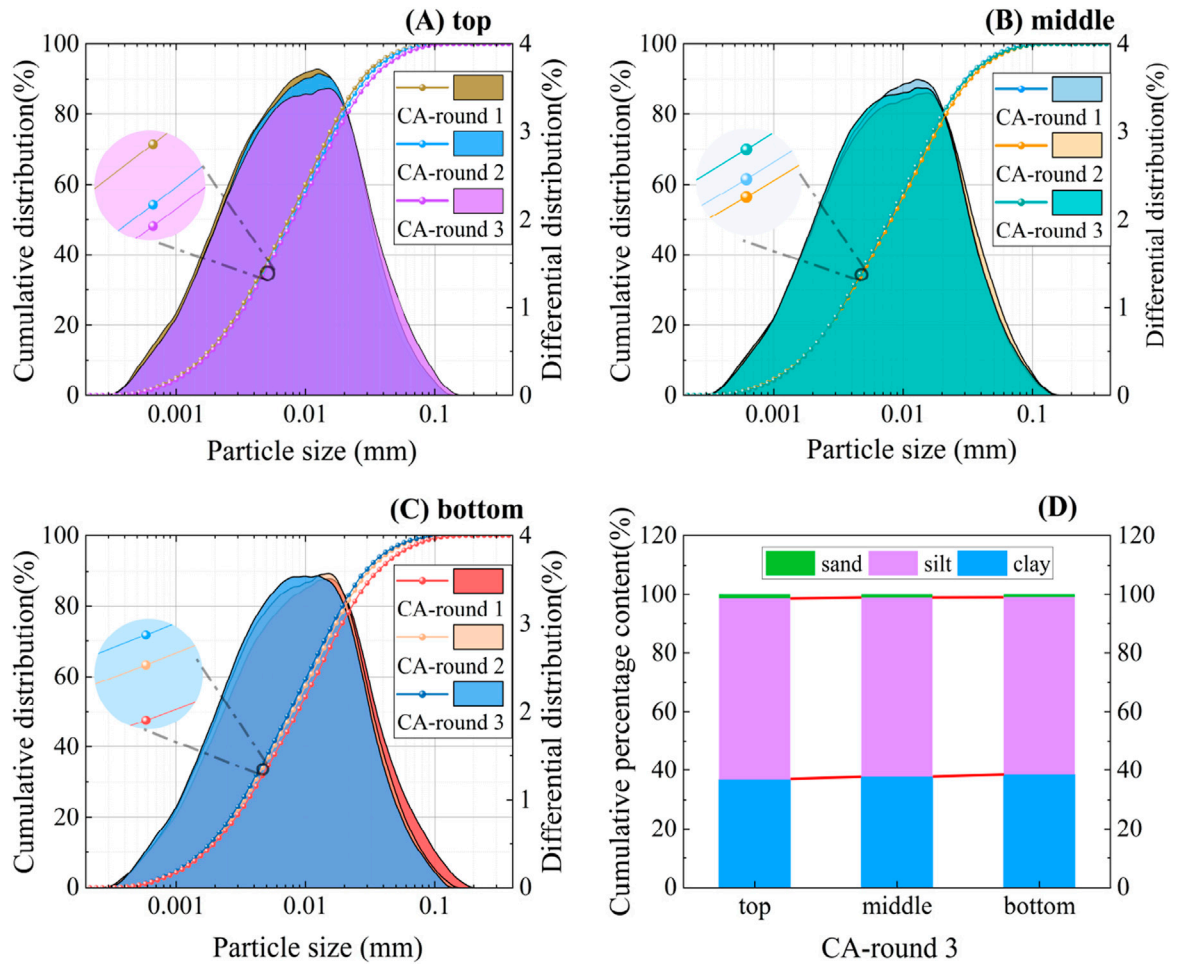

FIGURE 6
Particle distribution of soil samples at the same location for different leaching rounds **(A)**: top, **(B)**: middle, **(C)**: bottom, **(D)**: CA-round 3 particle distribution.

it was more obvious that with leaching rounds increased, the soil microstructure became looser, fine particles increased, and there were more pores, indicating the strong corrosive impact of citric acid leaching. Thus, the aforementioned pattern of the permeability coefficient occurred. At the same time, a distinctive needle-stick structure emerged. As the number of leaching rounds increases and the reaction continues, the structures become more pronounced and more numerous. This structure mainly originated from the chemical action of citric acid, its acidic qualities and strong complexing ability, and this reaction prompted the recombination and precipitation of internal substances in the soil, which led to the formation of a unique needle-cluster morphology. The needle-stick structures act as miniature supporting skeletons, interspersed between the soil particles, providing additional support to the soil mass. Remarkably, in Figures 7M–P, the 5,000 × SEM images show significant agglomeration of the soil particles where these substances occur, suggesting that the cluster structure has a positive effect on the agglomeration of the soil particles. In addition, it has been found that such structures are gel particles, which are associated with an increased content of silica, as a result of the change in mineral composition after drenching, and it has been noted that such substances help to stabilize the structure (Wen et al., 2022).

3.3.3 Mineral compositions

Citric acid, as an external substance, greatly changed the pore fluid environment of the contaminated soils during leaching, then altered the mineral content of the soil (Ke et al., 2022). The top part of the soil was in direct contact with the leaching agent, resulting in the highest concentration of the agent in the pore fluid, the XRD analysis results were shown in Figure 8. The data in the figure are the average of the experiments.

Quartz constituted the primary component in the soil both pre- and post-leaching, with a concentration exceeding 50%, showing a gradual rise with each subsequent leaching cycle. The content of chlorite also increased with the increase in leaching. attributed to the transformation of illite into chlorite in a Mg^{2+}-rich environment (Jie et al., 2017). The acidic environment of citric acid would cause the Ca^{2+} and Mg^{2+} on the dolomite and calcite surface to be desorbed and free from pore fluid, creating favorable conditions for the illite transformation, so the illite content steadily declined to 5.3%. A related study (Ke et al., 2022) showed that illite and feldspar minerals

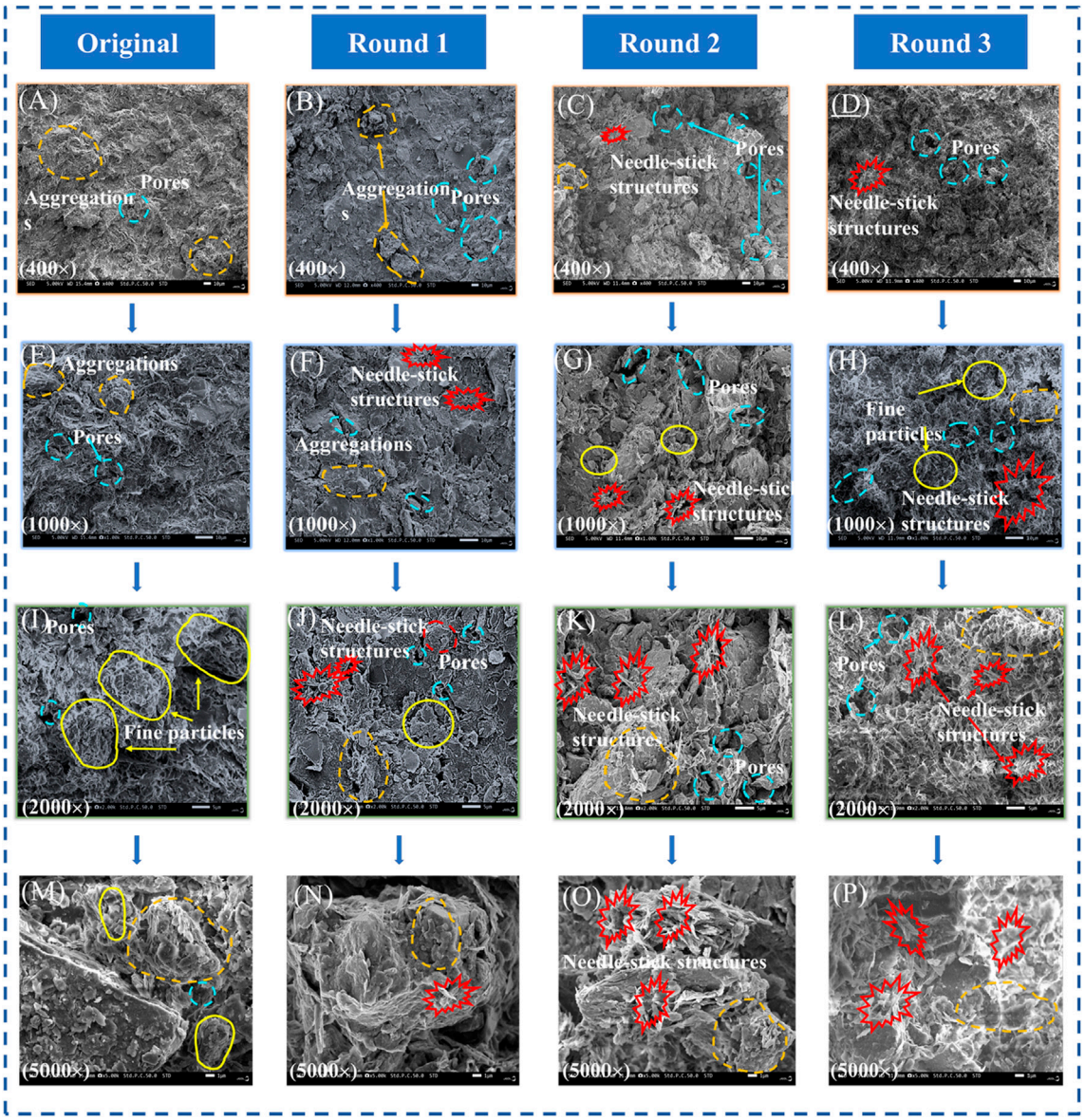

FIGURE 7
SEM images of soil samples with different leaching rounds at different scales **(A,E,I,M)**: original contaminated soil, **(B,F,J,N)**: CA-round 1, **(C,G,K,O)**: CA-round 2, **(D,H,L,P)**: CA-round 3.

were dissolved in an acidic environment and produced SiO_2, Al_2O_3, Fe_2O_3, etc., so the content of quartz and hematite increased. The feldspar mineral content decreased overall with each leaching round, although there was a slight increase in the first round likely due to insufficient acidification, so there was no significant dissolution, but rather, some albite was formed under the environmental conditions (Meng et al., 2023). With the increase in leaching, the soil environment was gradually acidified, the dissolution of feldspar minerals intensified, and the content decreased.

4 Discussion

The study researched the effects of leaching rounds on the contaminated soil remediation from the macro and micro levels, and provides multi-dimensional support for future engineering applications. The following are the specific conclusions.

(1) Bottom vacuum combined with citric acid multiple leaching technology was proposed, two rounds of leaching can meet the remediation requirements (removal rate) and three rounds can achieve a high removal rate of 85.0% ± 0.5% for Cu and 89.1% ± 0.3% for Zn. It solved the problem of poor remediation effect of low permeability contaminated clay, and provided a pioneering way for *in-situ* leaching of contaminated sites.
(2) The soil samples' geotechnical properties changed significantly after remediation. It was found that increasing leaching rounds would promote a rise in the void ratio, permeability, consolidation and compression coefficient,

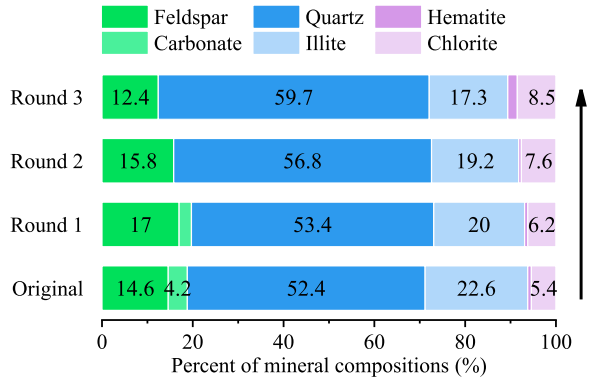

FIGURE 8
XRD results and analysis with different leaching rounds.

and these properties showed phased changes at loading. The effect of leaching rounds on each soil layer also varied. This experiment further improved the evaluation of remediated contaminated soil properties based on promoting the remediation effect.

(3) In this experiment, the remediation effect was evaluated in multiple dimensions, both macroscopic and microscopic. With the leaching rounds increasing, the corrosive effect of citric acid was more significant, the soil micro-structure became looser with more fine particles, a finding that corroborated the increase in Cu and Zn removal. Meanwhile, the pore structure became larger, as evidenced by an increase in void ratio. The emergence of the needle-stick structure favored soil agglomeration, which ultimately increased the permeability, consolidation and compression coefficients. This discovery explored the microscopic mechanism of leaching remediation.

Data availability statement

The original contributions presented in the study are included in the article/Supplementary Material, further inquiries can be directed to the corresponding author.

Author contributions

XZ: Conceptualization, Data curation, Formal Analysis, Funding acquisition, Project administration, Resources, Writing – review and editing. YZ: Conceptualization, Data curation, Formal Analysis, Investigation, Methodology, Writing – original draft, Writing – review and editing. HY: Conceptualization, Data curation, Formal Analysis, Supervision, Validation, Writing – review and editing.

Funding

The author(s) declare that financial support was received for the research and/or publication of this article. The authors are grateful for the support from Science and Technology Innovation Action Plan International Science and Technology Cooperation Project (22230730900).

Conflict of interest

Author XZ was employed by Shanghai Yaxin Urban Construction Co., Ltd.

The remaining authors declare that the research was conducted in the absence of any commercial or financial relationships that could be construed as a potential conflict of interest.

Generative AI statement

The author(s) declare that no Generative AI was used in the creation of this manuscript.

Publisher's note

All claims expressed in this article are solely those of the authors and do not necessarily represent those of their affiliated organizations, or those of the publisher, the editors and the reviewers. Any product that may be evaluated in this article, or claim that may be made by its manufacturer, is not guaranteed or endorsed by the publisher.

References

Antoniadis, V., Levizou, E., Shaheen, S. M., Sik Ok, Y., Sebastian, A., Baum, C., et al. (2017). Trace elements in the soil-plant interface: phytoavailability, translocation, and phytoremediation-A review. *Earth-Science Rev.* 171, 621–645. doi:10.1016/j.earscirev.2017.06.005

Aria, N., Eris, U., and Zalihe, N. (2022). A review on the effects of landfill leachate on the physical and mechanical properties of compacted clay liners for municipality landfills. *Arabian J. Geosciences* 15, 1174. doi:10.1007/s12517-022-10430-w

Chen, Y., Zhang, S., Xu, X., Yao, P., Li, T., Wang, G., et al. (2016). Effects of surfactants on low-molecular-weight organic acids to wash soil zinc. *Environ. Sci. Pollut. Res.* 23, 4629–4638. doi:10.1007/s11356-015-5700-3

Covelo, E. F., Vega, F. A., and Andrade, M. L. (2007). Simultaneous sorption and desorption of Cd, Cr, Cu, Ni, Pb, and Zn in acid soils: I. Selectivity sequences. *J. Hazard. Mater.* 147, 852–861. doi:10.1016/j.jhazmat.2007.01.123

Cui, P., Wen, G. C., Xu, Z., Wei, Y., and Huixin, L. (2023). One-dimensional non-linear rheological consolidation of clayey soils with Swartzendruber's flow law. *Comput. Geotechnics* 155, 105201. doi:10.1016/j.compgeo.2022.105201

Cyriac, J., Sreejit, C. M., Yuvaraj, M., Joseph, S., Sathya Priya, R., Saju, F., et al. (2024). Zinc-exchanged montmorillonite clay: a promising slow-release nanofertilizer for rice (Oryza sativa L.). *Plant Physiology Biochem.* 212, 108790. doi:10.1016/j.plaphy.2024.108790

Elkateb, T. (2017). Stress-dependent consolidation characteristics of marine clay in the Northern Arabian Gulf. *Ain Shams Eng. J.* 9, 2291–2299. doi:10.1016/j.asej.2017.05.001

Guo, G., Chen, S., Lei, M., Wang, L., Yang, J., and Qiao, P. (2023). Spatiotemporal distribution characteristics of potentially toxic elements in agricultural soils across China and associated health risks and driving mechanism. *Sci. total Environ.* 887, 163897–97. doi:10.1016/j.scitotenv.2023.163897

Han, J., Zou, J., Li, X., Ding, A., Shang, Z., Sun, H., et al. (2024). Study on the remediation of uranium-contaminated soils by compound leaching: screening of leaching agents and a pilot-scale application. *J. Clean. Prod.* 450, 141918. doi:10.1016/j.jclepro.2024.141918

Hao, Lu T., Sun, W. J., Liu, K., and Tan, Y. Z. (2022). Effect of sand particle size on hydraulic-mechanical behavior of bentonite-sand mixtures. *KSCE J. Civ. Eng.* 26, 3287–3300. doi:10.1007/s12205-022-1271-2

Hong, Z. S., Yin, J., and Cui, Y. J. (2010). Compression behaviour of reconstituted soils at high initial water contents. *Géotechnique* 60, 691–700. doi:10.1680/geot.09.P.059

Hu, W., Niu, Y., Zhu, H., Dong, K., Wang, D., and Liu, F. (2021). Remediation of zinc-contaminated soils by using the two-step washing with citric acid and water-soluble chitosan. *Chemosphere* 282, 131092. doi:10.1016/j.chemosphere.2021.131092

Indraratna, B., Bamunawita, C., and Khabbaz, H. (2004). Numerical modeling of vacuum preloading and field applications. *Can. Geotechnical J.* 41, 1098–1110. doi:10.1139/T04-054

Indraratna, B., Kan, M. E., Potts, D., Rujikiatkamjorn, C., and Sloan, S. W. (2016). Analytical solution and numerical simulation of vacuum consolidation by vertical drains beneath circular embankments. *Comput. and Geotechnics* 80, 83–96. doi:10.1016/j.compgeo.2016.06.008

Jez, E., and Lestan, D. (2016). EDTA retention and emissions from remediated soil. *Chemosphere* 151, 202–209. doi:10.1016/j.chemosphere.2016.02.088

Jie, M., Benxian, L. I., Zhang, J., and Liu, X. (2017). Patterns of clay minerals transformation in clay gouge, with examples from revers fault rocks in Devonina Niqiuhe formation in the dayangshu basin. *Acta Geol. Sin. Ed.* 91, 59–60. doi:10.1111/1755-6724.13185

Jongkwan, K., Motoki, K., and Kawai, T. (2021). Evaluation of post-liquefaction volumetric strain of reconstituted samples based on soil compressibility. *Soils Found.* 61, 1555–1564. doi:10.1016/j.sandf.2021.09.002

Kamal, A. A., Mahmood, A. K., and Duja, S. (2021). Remediation of clayey soil contaminated with nickel nitrate using enhanced electro-kinetics process and study the geotechnical properties of the remediated soil samples. *Mater. Today Proc.* 42, 2516–2520. doi:10.1016/j.matpr.2020.12.572

Ke, X., Zhang, F. J., Zhou, Y., Zhang, H. J., Guo, G. L., and Yu, T. (2020). Removal of Cd, Pb, Zn, Cu in smelter soil by citric acid leaching. *Chemosphere* 255, 126690. doi:10.1016/j.chemosphere.2020.126690

Ke, Z., Feng, B., Liu, Y., Cui, Z., and Liu, X. (2022). Dissolution and sedimentation patterns of typical minerals in artificial reservoirs under different environments. *Unconv. Resour.* 2, 60–71. doi:10.1016/j.uncres.2022.08.004

Kuśmierz, S., Skowrońska, M., Tkaczyk, P., Lipiński, W., and Mielniczuk, J. (2023). Soil organic carbon and mineral nitrogen contents in soils as affected by their pH, texture and fertilization. *Agronomy* 13, 267. doi:10.3390/agronomy13010267

Kwangkyun, K., Park, D., Kwon, Y. J., and Lee, J. (2013). Permeability and consolidation characteristics of clayey sand soils. *J. Korean Geotechnical Soc.* 29 (3), 61–70. doi:10.7843/kgs.2013.29.3.61

Lei, H., Lu, H., Liu, J., and Zheng, G. (2017). Experimental study of the clogging of dredger fills under vacuum preloading. *Int. J. Geomechanics* 17. doi:10.1061/(asce)gm.1943-5622.0001028

Li, J., Xue, Q., Wang, P., and Li, Z. (2015). Effect of lead (II) on the mechanical behavior and microstructure development of a Chinese clay. *Appl. Clay Sci.* 105, 192–199. doi:10.1016/j.clay.2014.12.030

Li, Y., Liu, J., Wang, Y., Tang, X., Xu, J., and Liu, X. (2023). Contribution of components in natural soil to Cd and Pb competitive adsorption: semi-quantitative to quantitative analysis. *J. Hazard. Mater.* 441, 129883. doi:10.1016/j.jhazmat.2022.129883

Li, Y., Lou, J., Wang, H., Wu, L., and Xu, L. (2018). Use of an improved high-throughput absolute abundance quantification method to characterize soil bacterial community and dynamics. *Sci. Total Environ.* 633, 360–711. doi:10.1016/j.scitotenv.2018.03.201

Liao, X., Li, Y., Miranda-Aviles, R., Zha, X., Anguiano, J. H. H., Sanchez, C. D. M., et al. (2022). *In situ* remediation and *ex situ* treatment practices of arsenic-contaminated soil: an overview on recent advances. *J. Hazard. Mater. Adv.* 8, 100157. doi:10.1016/j.hazadv.2022.100157

Lin, L., Han, S., Pengzhi, Z., Lu, L., Zhang, C., and Wang, E. (2022). Influence of soil physical and chemical properties on mechanical characteristics under different cultivation durations with mollisols. *Soil and Tillage Res.* 224, 105520. doi:10.1016/j.still.2022.105520

Liu, F., Yi, S., Zhou, W., Chen, Y., and Wong, M. (2021). Amendment additions and their potential effect on soil geotechnical properties: a perspective review. *Crit. Rev. Environ. Sci. Technol.* 51, 535–576. doi:10.1080/10643389.2020.1729066

Liu, H., Chen, P., Wang, H., Yang, Y., and Wu, Y. (2023). Remediation of Cu-Zn-and Pb-contaminated soil using different soil washing agents: removal efficiencies and mechanisms. *Water, Air, and Soil Pollut.* 234, 476. doi:10.1007/s11270-023-06463-w

Liu, J., Lei, H., Zheng, G., Feng, S., and Rahman, M. S. (2018). Improved synchronous and alternate vacuum preloading method for newly dredged fills: laboratory model study. *Int. J. Geomechanics* 18. doi:10.1061/(asce)gm.1943-5622.0001220

Mejlhede, K. E., Ole, H., Irene, R., and Varvara, Z. (2023). Primary and secondary consolidation characteristics of a high plasticity overconsolidated clay in compression and swelling. *Soils Found.* 63, 101375. doi:10.1016/j.sandf.2023.101375

Meng, W., Sui, F., Zhang, T., Hao, X., Wu, Y., Jiang, Y., et al. (2023). Thermodynamic mechanism and its geological significance in the transformation of albite under inorganic acid environments based on the total dissolution model. *Geoenergy Sci. Eng.* 221, 111295. doi:10.1016/j.petrol.2022.111295

Novikau, R., and Lujaniene, G. (2022). Adsorption behaviour of pollutants: heavy metals, radionuclides, organic pollutants, on clays and their minerals (raw, modified and treated): a review. *J. Environ. Manag.* 309, 114685. doi:10.1016/j.jenvman.2022.114685

Oliveira, C., Jr, and Massao, F. M. (2015). Influence of mineralogy and microstructure on the mechanical behavior of a gneissic residual soil. *Stand Alone* 0, 2630–2637. doi:10.3233/978-1-61499-603-3-2630

Raza, S., Zamanian, K., Ullah, S., Kuzyakov, Y., Virto, I., and Zhou, J. (2021). Inorganic carbon losses by soil acidification jeopardize global efforts on carbon sequestration and climate change mitigation. *J. Clean. Prod.* 315, 128036. doi:10.1016/j.jclepro.2021.128036

Rehman, Z. U., Junaid, M. F., Ijaz, N., Khalid, U., and Ijaz, Z. (2023). Remediation methods of heavy metal contaminated soils from environmental and geotechnical standpoints. *Sci. Total Environ.* 867, 161468. doi:10.1016/j.scitotenv.2023.161468

Saowapakpiboon, J., Bergado, D. T., Voottipruex, P., Lam, L. G., and Nakakuma, K. (2011). PVD improvement combined with surcharge and vacuum preloading including simulations. *Geotextiles and Geomembranes.* 29, 74–82. doi:10.1016/j.geotexmem.2010.06.008

Sheng, Y., Liang, T., Xian, L., and Sai, K. (2025). Insights into the shallow landslide mechanism of expansive soil slope induced by freeze–thaw cycles and snowmelt infiltration. *Can. Geotech. J.* 62, 1–17. doi:10.1139/cgj-2024-0041

Shentu, J., Fang, Y., Wang, Y., Cui, Y., and Zhu, M. (2023). Bioaccessibility and reliable human health risk assessment of heavy metals in typical abandoned industrial sites of southeastern China. *Ecotoxicol. Environ. Saf.* 256, 114870. doi:10.1016/j.ecoenv.2023.114870

Tang, M., and Shang, J. Q. (2000). Vacuum preloading consolidation of Yaoqiang airport runway. *Géotechnique* 50, 613–623. doi:10.1680/geot.2000.50.6.613

Wang, P., Huang, X., Li, W., Wang, K., Chen, Z., and Liu, H. (2024). Enhanced consolidation and removal of accumulated flocculants in dredged soil via leaching with vacuum preloading. *Environ. Geochem. Health* 46, 286. doi:10.1007/s10653-024-02067-3

Wang, Z., Wang, H., Wang, H., Li, Q., and Yang, L. (2020). Effect of soil washing on heavy metal removal and soil quality: a two-sided coin. *Ecotoxicol. Environ. Saf.* 203, 110981. doi:10.1016/j.ecoenv.2020.110981

Wen, W., Jia, L., Xie, J., Zhao, W., Feng, H., Cao, D., et al. (2022). Electrochemical response of solidification Cu^{2+} contaminated soil influenced by red mud/fly ash ratio. *Heliyon* 8, e10971. doi:10.1016/j.heliyon.2022.e10971

Wu, J., Yang, N., Li, P., and Yang, C. (2023). Influence of moisture content and dry density on the compressibility of disturbed loess: a case study in Yan'an city, China. *Sustainability* 15, 6212. doi:10.3390/su15076212

Wu, Y., Sun, Y., Zhang, X., Zhang, H., Ye, P., He, K., et al. (2022a). Experiments and mechanisms for bottom vacuum leaching remediation of low permeability Cu, Zn-contaminated soil. *J. Clean. Prod.* 367, 133038. doi:10.1016/j.jclepro.2022.133038

Wu, Y., Wang, X., Zhang, X., Lu, Y., Chen, M., Sun, Y., et al. (2022b). Experimental study on remediation of low permeability Cu-Zn contaminated clay by vacuum enhanced leaching combined with EDTA and hydrochloric acid. *Chemosphere* 298, 134332. doi:10.1016/j.chemosphere.2022.134332

Xie, N., Chen, Z., Wang, H., and You, C. (2021). Activated carbon coupled with citric acid in enhancing the remediation of Pb-Contaminated soil by electrokinetic method. *J. Clean. Prod.* 308, 127433. doi:10.1016/j.jclepro.2021.127433

Xu, Y., Liang, X., Xu, Y., Qin, X., Huang, Q., Wang, L., et al. (2017). Remediation of heavy metal-polluted agricultural soils using clay minerals: a review. *Pedosphere* 27, 193–204. doi:10.1016/S1002-0160(17)60310-2

Yan, K., Wang, H., Lan, Z., Zhou, J., Fu, H. Z., Wu, L., et al. (2022). Heavy metal pollution in the soil of contaminated sites in China: research status and pollution assessment over the past two decades. *J. Clean. Prod.* 373, 133780. doi:10.1016/j.jclepro.2022.133780

Yang, Z., Zhang, K., Li, X., Chang, J., Yang, S., and Ran, C. (2023). Mechanical and microstructural evolution of solidified/stabilized heavy metal-contaminated soil under a hydro-chemical-mechanical coupling environment. *Environ. Technol. and Innovation* 32, 103438. doi:10.1016/j.eti.2023.103438

Yu, Z., Ning, W., and Zhang, D. (2022). Research on nanoeffect of penetration and consolidation under nonlinear characteristics of saturated soft clay. *Int. J. Anal. Chem.* 2022, 7463817–17. doi:10.1155/2022/7463817

Zaki, A. A., Ahmad, M. I., and Abd El-Rahman, K. M. (2017). Sorption characteristics of a landfill clay soil as a retardation barrier of some heavy metals. *Appl. Clay Sci.* 135, 150–167. doi:10.1016/j.clay.2016.09.016

Zhang, J., Yao, B., Sun, Y., Wang, M., Qi, S., Sun, C., et al. (2022). Study of the effects of an ionic stabilizer on the permeability of gangue bonding material. *Constr. Build. Mater.* 345, 128325. doi:10.1016/j.conbuildmat.2022.128325

Zhang, X., Huang, T., Ge, Z., Man, T., and Huppert, E. (2025). Infiltration characteristics of slurries in porous media based on the coupled Lattice-Boltzmann discrete element method. *Comput. Geotech.* 17, 10266–352X. doi:10.1016/j.compgeo.2024.106865

Zhang, X., Ye, P., Wu, Y., and Zhai, E. (2022). Experimental study on simultaneous heat-water-salt migration of bare soil subjected to evaporation. *J. Hydrology* 609, 127710. doi:10.1016/j.jhydrol.2022.127710

Zheng, X. J., Qi, L., Peng, H., Zhang, J. X., Chen, W. J., Zhou, B. C., et al. (2022). Remediation of heavy metal-contaminated soils with soil washing: a review. *Sustainability* 14, 13058–58. doi:10.3390/su142013058

Zuo, T., Li, X., Wang, J., Hu, Q., Tao, Z., and Hu, T. (2024). Insights into natural tuff as a building material: effects of natural joints on fracture fractal characteristics and energy evolution of rocks under impact load. *Eng. Fail. Anal.* 163, 108584. doi:10.1016/j.engfailanal.2024.108584